Induction of Autophagy and Inhibition of Melanoma Growth *In Vitro* and *In Vivo* by Hyperactivation of Oncogenic BRAF

Nityanand Maddodi[1], Wei Huang[2], Thomas Havighurst[3], KyungMann Kim[3], B. Jack Longley[1] and Vijayasaradhi Setaluri[1]

Activating mutations in *NRAS* and *BRAF* are found frequently in cutaneous melanomas. Because concurrent mutations of both *BRAF* and *RAS* are extremely rare, it is thought that transformation by RAS and BRAF occurs through a common mechanism. Also, there is evidence for a relationship of synthetic lethality between *NRAS* and *BRAF* oncogenes that leads to selection against cells with a hyperactive mitogen-activated protein kinase (MAPK) pathway. However, it is not known whether the hyperactivation of the MAPK pathway by overexpression of either oncogene alone could also inhibit melanoma tumorigenesis. Here, we show that in melanoma cells with oncogenic BRAF (mBRAF), high levels of mBRAF induce hyperactivation of ERK and senescence-like phenotype and trigger autophagy by inhibiting the mammalian target of rapamycin complex signaling. Growth inhibition and cell death caused by high mBRAF levels are partially rescued by downregulation of BRAF protein or inhibition of autophagy, but not by inhibition of the MAPK or apoptotic pathways. In nude mice, growth of mBRAF-overexpressing tumors is inhibited. Quantitative immunohistochemical analysis of human melanomas and cell lines showed a significant positive correlation between the levels of BRAF protein and autophagy marker light chain 3. Our data suggest that high oncogenic BRAF levels trigger autophagy, which may have a role in melanoma tumor progression.

Journal of Investigative Dermatology (2010) **130,** 1657–1667; doi:10.1038/jid.2010.26; published online 25 February 2010

INTRODUCTION

Activating mutations in RAS and the RAS effector BRAF, which activate the mitogen-activated protein kinase (MAPK) signaling pathway, are found in a majority of melanomas (Demunter *et al.*, 2001; Davies *et al.*, 2002; Solit *et al.*, 2006). As the concurrent mutations of both BRAF and RAS are extremely rare, it is thought that transformation by RAS and BRAF occurs through a common mechanism involving the MEK-ERK signaling cascade (Sensi *et al.*, 2006). However, the specific role of oncogenic BRAF in melanoma remains to be understood (Karreth *et al.*, 2009). For example, it has been shown that BRAF is not required for MAPK activation in RAS-transformed melanocytes (Wellbrock *et al.*, 2004; Dumaz *et al.*, 2006). Although melanoma cell lines with activating mutation in BRAF are more sensitive *in vitro* to MEK inhibition than RAS mutant cell lines (Solit *et al.*, 2006), there was no correlation *in vivo* between the activation status of BRAF and the proportion of phosphor-ERK-positive cells or clinical course of the disease (Uribe *et al.*, 2006). Moreover, sorafenib, a multikinase inhibitor that also inhibits BRAF kinase, has little or no antitumor activity in advanced melanoma patients as a single agent (Eisen *et al.*, 2006).

Paradoxically, hyperactivation of RAS or BRAF and high levels of MAPK activities are also known to induce senescence and inhibit cell proliferation (Serrano *et al.*, 1997; Braig and Schmitt, 2006). In both the *in vitro* and *in vivo* model systems, activated BRAF has been shown to induce only nonmalignant changes in melanocytes, consistent with the hypothesis that BRAF induces a biphasic cellular response, i.e., an initial proliferative burst followed by senescence (Michaloglou *et al.*, 2005; Dankort *et al.*, 2007). Thus, a majority of benign melanocytic nevi, which harbor activating BRAF mutations, also exhibit hallmarks of senescence (Michaloglou *et al.*, 2005), suggesting that there may be an upper threshold for MAPK activation above which senescence is reactivated even in tumor cells. Thus, in human melanoma cells that carry mutant $NRAS^{Q61R}$, expression of $BRAF^{V600E}$ activates senescence, suggesting a relationship of synthetic lethality between the NRAS and BRAF oncogenes

[1]*Department of Dermatology, UW School of Medicine and Public Health, University of Wisconsin, Madison, Wisconsin, USA;* [2]*Department of Pathology, UW School of Medicine and Public Health, University of Wisconsin, Madison, Wisconsin, USA and* [3]*Department of Biostatistics, UW School of Medicine and Public Health, University of Wisconsin, Madison, Wisconsin, USA*

Correspondence: Vijayasaradhi Setaluri, Department of Dermatology, University of Wisconsin, B25 Dermatology Research, 1300 University Avenue, Madison, Wisconsin 53706, USA. E-mail: setaluri@wisc.edu

Abbreviations: AQUA, automated quantitative immunohistochemistry; BFA, brefeldin A; BRAF, v-raf murine sarcoma viral oncogene homolog B1; DAPI, 4,6-diamidino-2-phenylindole; ERK, extracellular signal-regulated kinase; MAP2, microtubule-associated protein 2; MAPLC3, microtubule-associated protein light chain 3; MTT, [3-(4,5-dimethyl thiazol-2-yl)-2,5-diphenyl tetrazolium bromide]; mTOR, mammalian target of rapamycin; NRAS, neuroblastoma RAS viral (v-ras) oncogene homolog; 4-OHT, 4-hydroxytamoifen; ZVAD-fmk, (carbobenzoxy-valyl-alanyl-aspartyl-[O-methyl]-fluoromethylketone)

Received 29 July 2009; revised 23 December 2009; accepted 3 January 2010; published online 25 February 2010

that results in selection against cells with a hyperactive MAPK pathway (Petti *et al.*, 2006). Although it is known that additional genetic changes are required for cellular escape from BRAF-induced senescence (Michaloglou *et al.*, 2005; Patton *et al.*, 2005; Dankort *et al.*, 2009) and that activated BRAF is required for tumor growth and maintenance (Hoeflich *et al.*, 2006), the relationship between the BRAF oncogene dosage and melanoma tumor progression and its responsiveness to treatment with BRAF kinase inhibitors is not known.

Here, we show that high mBRAF expression not only inhibits cell growth and triggers autophagy by inhibiting mTOR signaling, but also inhibits tumor growth *in vivo* by hemorrhagic necrosis. In human melanoma cell lines and tumor tissues, expression levels of BRAF protein showed a positive correlation with a marker of autophagy. These findings suggest a role for BRAF dosage-dependent autophagy in melanoma development and progression.

RESULTS

Overexpression of BRAF^{V600E} inhibits growth of melanoma cells

A survey of a representative panel of primary and metastatic human melanoma cell lines with wild-type or mutant RAS or BRAF alleles showed that although melanoma cell lines have nearly three- to fivefold more BRAF protein and RAF kinase activity compared with cultured melanocytes, there was no clear correlation between the BRAF mutation status or BRAF expression levels and the RAF kinase activity or pERK1/2 (see Supplementary Data, Supplementary Figure S1 online). For example, metastatic melanoma cell lines 451Lu harboring the mutant BRAF allele and SK-MEL-2 carrying a mutation in RAS have similar levels of BRAF protein, RAF kinase activity, and pERK. To investigate the effect of hyperstimulation of the MAPK pathway in melanoma cells, we transfected oncogenic BRAF^{V600E} (mBRAF) expression plasmid into melanoma cell lines 451Lu and SK-MEL-2 and generated stable cell lines expressing nearly twofold more BRAF protein compared with vector-transfected cells (Figure 1a, left and Figure 2a). The two high-mBRAF 451Lu stable clones, mBRAF2 and mBRAF3, isolated from two separate transfections, showed a decreased rate of proliferation despite having increased pERK levels (Figure 1b, left; Supplementary Figure S2a and S2b). Similarly, in a stable clone of 451Lu transfected with an inducible expression plasmid ER-BRAF^{V600E}, a dose-dependent inhibition of growth was observed when mBRAF expression was increased (up to ~20%) by treatment with tamoxifen (Figure 1a and b, right, and Supplementary Figure S2c). Tamoxifen treatment had no effect on the growth of the parental 451Lu cells. In a clonogenic survival assay, 451Lu-mBRAF clones produced 50% fewer colonies than vector control cells (Figure 1c). To rule out the possibility that the stable clones represent clonally expanded, rare, and slow-growing G418-resistant variants of parental 451Lu melanoma cells, we studied the effect of transient overexpression of mBRAF in 451Lu cells as well as WM35 (a primary melanoma cell line that carries the mutant BRAF allele). Both WM35 and 451Lu cells showed significant growth inhibition similar to the stable clones (Supplementary Figure S3a). Transient expression of mBRAF in additional melanoma cells lines (SK-MEL-28, Hs294T, and WM115) also resulted in variable growth inhibition (Supplementary Figure S4), confirming that high mBRAF levels inhibit melanoma cell proliferation. Interestingly, overexpression of BRAF and high pERK levels did not inhibit the growth of melanoma cell line SK-MEL-2, which carries wild-type BRAF and mutant RAS gene (Figure 2a–c), suggesting that hyperactivation of the oncogenic BRAF and MAPK pathway in melanoma cells with activated BRAF, but not activated RAS, results in growth inhibition.

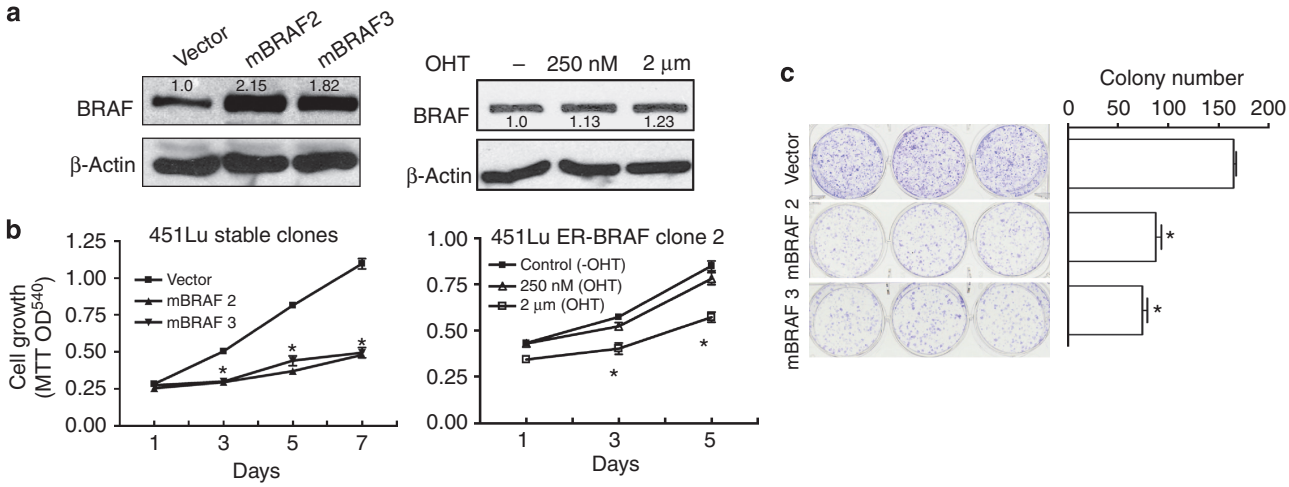

Figure 1. Overexpression of oncogenic BRAF inhibits growth. (**a**) 451Lu metastatic melanoma cells harboring BRAF V600E mutation were transfected with empty vector (pMCEFplink) or mBRAF (pMCEFBRAF^{V600E}) expression plasmid using Nucleofector (Amaxa) and two G418-resistant clones were selected from two separate transfections. Puromycin-resistant stable clones from empty vector or pLXSP3-G BRAF^{VE}:ER^{T2} plasmid transfections of 451Lu were generated. Cell lysates were analyzed by western blots using the anti-BRAF antibody. (Numbers below the bands indicate fold increase in BRAF protein.) Actin shows equal loading. (**b**) MTT assay for cell proliferation. Left: 451Lu-mBRAF clones; right: 4-OHT (4-hydroxytamoxifen)-inducible ER-mBRAF clone. Representative data from three independent experiments are shown (*$P<0.001$). (**c**) Colony-forming ability of 451Lu control and mBRAF clones. Cells (5000 per well) were plated in triplicate, and 2 weeks later crystal violet-stained colonies were counted. Representative data from three independent experiments are shown (*$P<0.001$).

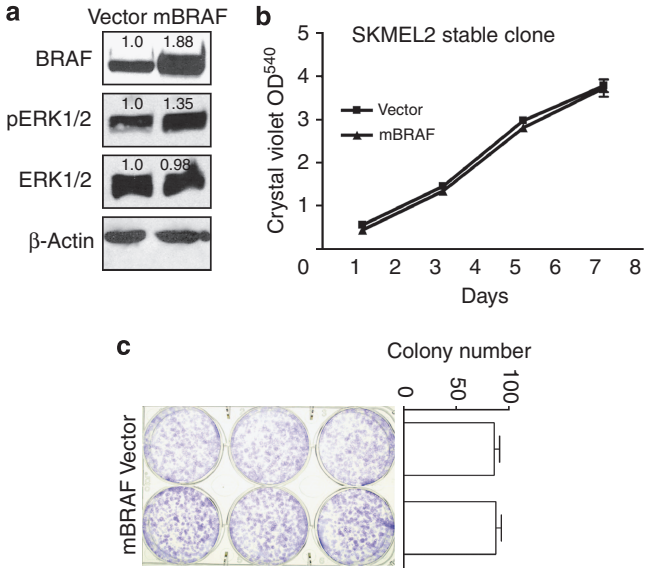

Figure 2. RAS mutant, BRAF wild-type SK-MEL-2 cells are refractory to oncogenic BRAF. (**a**) Western blot analysis vector control and stable mBRAF expressing SK-MEL-2 metastatic melanoma cells. Actin shows equal loading. (**b**) Cells (1×10^5) were plated in a six-well plate and growth was measured by crystal violet assay. (**c**) Clonogenicity of control and mBRAF SK-MEL-2 cells. Crystal violet-stained colonies were counted and the number of colonies is shown.

Hyperactivation of BRAF induces senescence-like features but not cell cycle arrest and apoptosis

As activated BRAF induces senescence in melanocytes, we asked whether high mBRAF levels can reactivate senescence in melanoma cells. We used senescence-associated-β-galactosidase, p16 expression, and acetylated histone H3 (AcH3K9) as markers of senescence. In 451Lu-mBRAF, we observed a threefold increase in senescence-associated-β-galactosidase stained-positive cells (Figure 3a), upregulation of p16 protein and a decrease in acetylated histone H3 (Figure 3b). Similar increase in senescence-associated-β-galactosidase-positive cells was seen in SK-MEL-2 mBRAF stable clone, and also in WM35 and 451Lu cells transiently transfected with mBRAF (Supplementary Figure S3b). Together, these data suggest that overexpression of mBRAF (re)activates senescence in both mutant RAS and mutant BRAF melanoma cells, whereas high BRAF levels only inhibit the growth of cells expressing endogenous $BRAF^{V600E}$.

To understand the mechanisms of growth inhibition by high mBRAF, we evaluated cell cycle distribution and TUNEL staining. In 451Lu-mBRAF cells, although there seems to be a small increase in the S-phase, there was no change in the proportion of cells in the G1 or G2/M phases of the cell cycle or the number of TUNEL-positive cells between vector and 451Lu-mBRAF clones (Figure 3c). Addition of 5 μM fmk-ZVAD, a pan-caspase inhibitor, to the culture medium did not rescue growth of 451Lu-mBRAF clones (Figure 3d). Treatment of vector control 451Lu cells with the same concentration of fmk-ZVAD modestly increased their survival (Figure 3d) and was sufficient to rescue, partially but significantly, tumor necrosis factor-α-induced apoptosis (Supplementary Figure S5). These data show that cell cycle arrest and apoptosis are not primary mechanisms of growth inhibition caused by high mBRAF levels.

High level of oncogenic BRAF induces autophagy

We asked whether autophagy, an alternative form of cell death, could account for the growth inhibition caused by mBRAF overexpression. First, immunofluorescence staining for the autophagy marker microtubule-associated protein light chain 3 (LC3, a mammalian homolog of Atg8, a yeast protein involved in autophagy) showed punctate staining of LC3-positive autophagic vesicles in mBRAF3 (Figure 4a, top). The specificity of LC3 staining was verified by a similar pattern of accumulation of transfected green fluorescent protein (GFP)–LC3 fusion protein (Kabeya *et al.*, 2000) in vesicles in 451Lu-mBRAF2 cells but not in control cells. Treatment with brefeldin A, an inducer endoplasmic stress and autophagy (Turcotte *et al.*, 2008), also produced a similar pattern of GFP–LC3 accumulation in vector control 451Lu cells (Figure 4a, lower) showing the prevalence of autophagosomes in mBRAF cells. Biochemically, the autophagosome-associated lipidated form of LC3 (LC3-II) can be distinguished from free LC3 (LC3-I) by immunoblotting (Kabeya *et al.*, 2000). Consistent with the morphological findings, a higher amount of lipidated LC3-II was seen in 451Lu-mBRAF clones (Figure 4a). Staining with the fluorescent dye monodansyl cadavarine, which labels large acidic autophagosome lysosomes (Supplementary Figure S6a), and transmission electron microscopy that showed characteristic double-membrane autophagic vesicles (Figure 4a) and numerous vacuoles (Supplementary Figure S6b) supported our data on activation of autophagy in melanoma cells overexpressing mBRAF.

Activation of autophagy in 451Lu-mBRAF cells raised the possibility that autophagic cell death might contribute to growth inhibition by high mBRAF. To test this, we treated control and mBRAF cells with 3-methyladenine (3-MA), an inhibitor of autophagy (Petiot *et al.*, 2000), and evaluated the proportion of dead cells. In untreated 451Lu-mBRAF clones, there were 2–3 times more dead cells compared with vector-transfected 451Lu cells. Treatment with 3-MA for 48 hours significantly reduced the number of dead cells in the mBRAF clone, whereas 3-MA treatment had no effect on control cells (Figure 4d). A reduction in the amount of lipidated LC3-II in 3-MA-treated cells verified inhibition of autophagy by 3-MA (Supplementary Figure S6c). Conversely, the MTT assay showed that treatment with 3-MA resulted in a small, but significant, increase in growth of mBRAF cells (Supplementary Figure S6d).

As mammalian target of rapamycin (mTOR) is known to regulate autophagy, we tested whether hyperactivation of BRAF modulates mTOR activity. Western blot analysis of components of the mTOR complexes (Figure 4e) showed an increase in phosphorylation of mTOR at Ser2481 and an increase in Rictor, which are associated with the rapamycin-insensitive mammalian target of rapamycin complex-2 (mTORC2). There was no marked change in phosphorylation at Ser2448 and the expression of Raptor, which, however, are

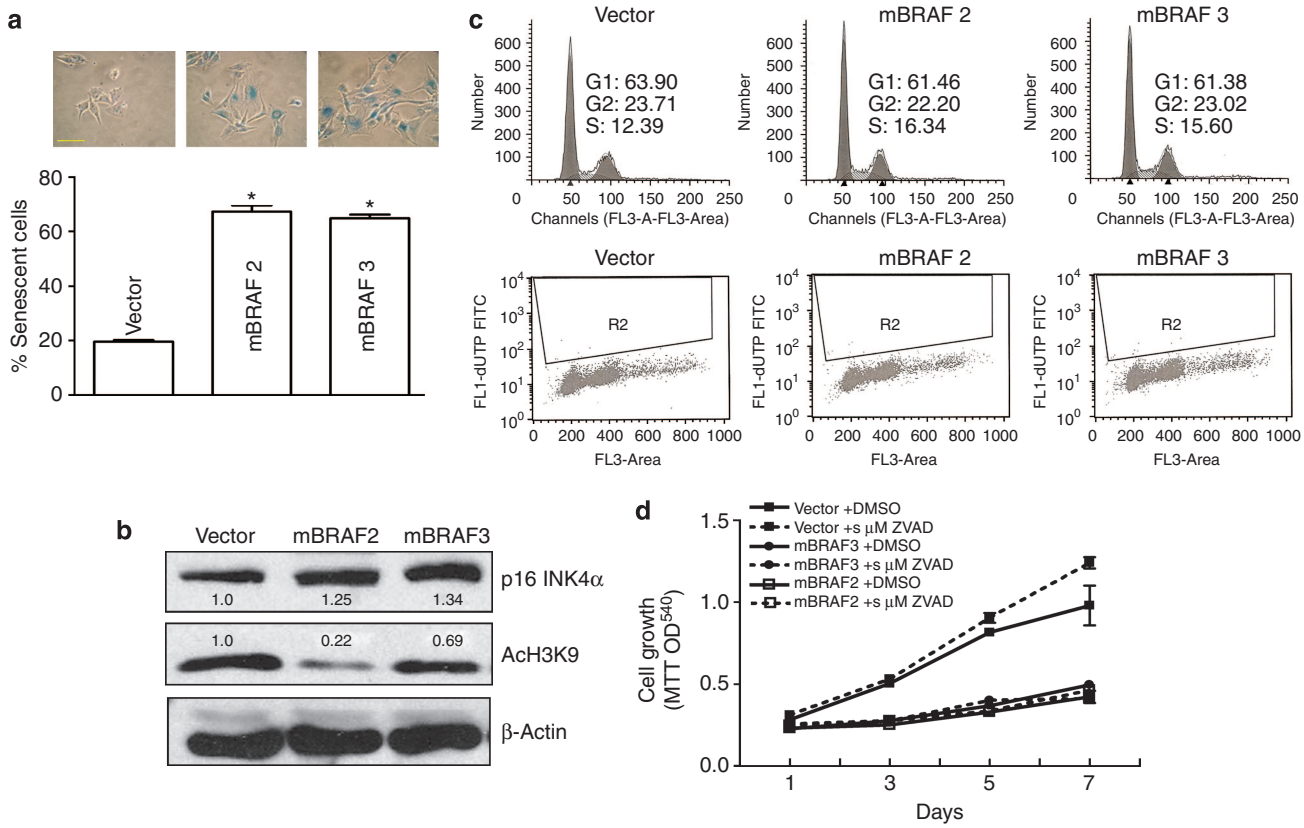

Figure 3. Hyperactivation of mBRAF induces senescence but not apoptosis in melanoma cells. (**a**) Cells (5,000 per well) were plated in triplicate and stained to detect senescence-associated-β-galactosidase (SA-β-gal) (insets), and percent SA-β-gal-positive cells were counted. Representative data from three independent experiments are shown (*$P<0.001$). (Bar = 4 mm). (**b**) Immunoblot analysis of $p16^{INK4A}$ and acetylated H3K9. Actin was used as a loading control. (**c**) Expression of mBRAF does not inhibit cell cycle. 451Lu vector and mBRAF-expressing cells were stained with propidium iodide and analyzed by flow cytometry for cell cycle distribution (upper) and TUNEL-positive cells (lower). (**d**) Inhibition of apoptosis does not rescue the growth of high mBRAF cells. Control and 451Lu-mBRAF cells were treated with pan-caspase inhibitor fmk-ZVAD, and cell survival was measured by MTT assay. Representative data from three independent experiments are shown.

associated with mTORC1 that negatively regulates autophagy (Copp *et al.*, 2009). Treatment of 451Lu vector control cells with autophagy-inducer brefeldin A also caused a similar increase in Rictor (lane 4, Figure 4e). Decreased signaling by mTORC1 in mBRAF cells is also indicated by reduced phospho-4E-BP1 (the translational repressor of eukaryotic elongation factor-binding protein) (Figure 4f). Similarly, phosphorylation of Akt at Thr308 and tuberin (TSC2) at Thr1462, both components upstream of mTORC1, is also decreased in mBRAF cells (Figure 4f). These data suggest that hyperactivation of BRAF inhibits Akt-mTORC1 signaling and thereby attenuates the negative regulation of autophagy by mTORC1. Thus, high levels of oncogenic BRAF appear to inhibit growth and induce autophagy-associated cell death by modulating the mTOR signaling pathway that is reported to be activated in the majority of melanomas (Karbowniczek *et al.*, 2009).

To test whether pharmacological inhibition of mTOR by rapamycin also induces autophagy and inhibits melanoma cell growth, we treated 451Lu cells with rapamycin (0.1–2 μM) and measured cell proliferation (by MTT assay) and induction of autophagy (by GFP-LC3 staining). As shown in Supplementary Figure S7, treatment with 2 μM rapamycin caused significant growth inhibition and vesicular accumulation of GFP-LC3, showing that inhibition of the rapamycin-sensitive mTORC1 leads to induction of autophagy in 451Lu melanoma cells.

Downregulation of BRAF inhibits autophagy

Next, we asked whether autophagy-associated growth inhibition by high mBRAF can be reversed by reducing BRAF levels. For this, we used BRAF small hairpin RNA (shRNA) lentiviral transduction followed by selection in puromycin. First, we titrated the virus and used a titer to achieve ~20% decrease in BRAF protein levels (Figure 5a). This level of BRAF knockdown in control 451Lu cells resulted in a small but significant decrease in growth. In contrast, a similar knockdown of BRAF in 451Lu-mBRAF cells resulted in a significant increase in growth (Figure 5b), suggesting that a high level of activated BRAF is required for growth suppression. Knockdown of BRAF also decreased senescence as indicated by the p16 levels (Figure 5c).

Infection with higher titers of BRAF shRNA lentivirus, which caused a further decrease (40–50%) in BRAF levels, significantly inhibited proliferation of both control and 451Lu-mBRAF cells (Supplementary Figure S8a and b), as

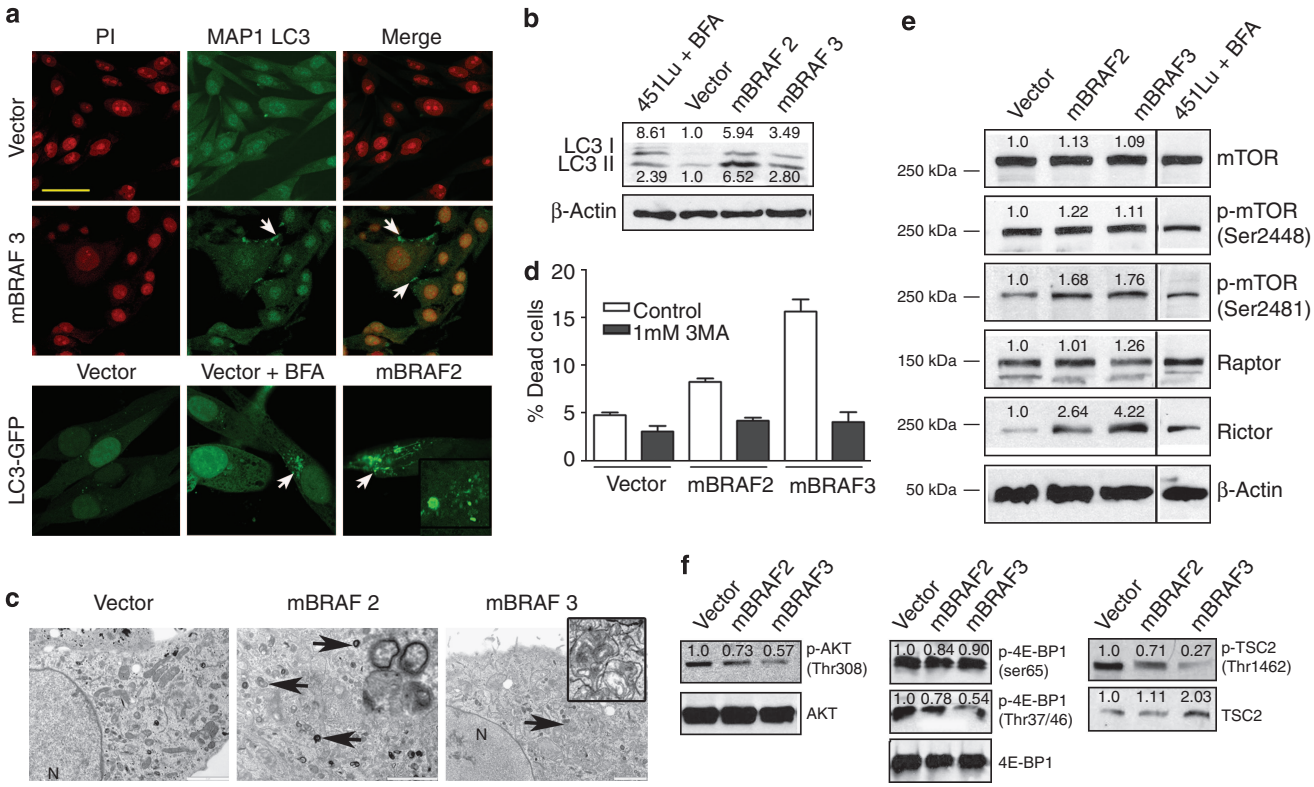

Figure 4. High level of oncogenic BRAF activates autophagy in melanoma cells. (**a**) Immunofluorescence staining of autophagic marker MAP1LC3 in 451Lu-mBRAF cells shows punctate staining of autophagic vesicles (arrows). Cells plated on cover glass were incubated with LC3 antibody followed by anti-mouse IgG-FITC and visualized in a confocal microscope. Nuclei were stained with propidium iodide (upper). Representative confocal images of GFP-LC3-transfected vector control 451Lu and control cells treated with 10 μM brefeldin A (BFA) and untreated 451Lu-mBRAF3 (lower). Arrows indicate GFP-LC3-positive autophagosomal structures. Inset shows higher magnification. (Bar = 50 μm). (**b**) Induction of autophagic marker LC3-II isoform in mBRAF-expressing cells. Western blot analysis of total cell lysate from 451Lu mBRAF, vector, and 451Lu treated with 10 μM BFA for 24 hours and probed with LC3 antibody. Actin was used as a loading control. (**c**) Transmission electron microscopy of control and mBRAF3 cells. Arrows and inset show double membrane autophagic vesicles. (Bar = 2 μm). (**d**) Inhibition of autophagy decreases cell death in mBRAF-expressing cells. Cells were treated with 1 mM 3MA and dead cells were measured after 24 hours using the Cytotox-glo assay kit. Representative data (mean ± SEM) from three independent experiments are shown. (**e**) Western blot analysis of mTORC1 and mTORC2 complexes in vector control, mBRAF2 and -3 clones, and BFA-treated 451Lu cells. Numbers on the left indicate the position of molecular weight markers. (Numbers below the bands indicate densitometric quantitation of the bands normalized to actin). (**f**) Western blot analysis of upstream and downstream targets of mTORC1 complex in vector control, and mBRAF2 and -3 clones.

expected, showing that a threshold level of BRAF is required for survival of melanoma cells, whereas high BRAF levels are growth inhibitory.

Next, we tested whether sustained high activation of BRAF downstream effector MEK is also required for growth suppression by high mBRAF. We treated cells with MEK inhibitor U0126 at a concentration (0.5 μM) that inhibits the growth of control 451Lu cells by 30% after a 7-day treatment. A similar treatment, however, did not significantly affect the survival or growth of 451Lu-mBRAF cells (Figure 5d). Western blot analysis did not reveal a marked difference in the degree of inhibition of ERK1/2 phosphorylation by U0126 in vector control compared with mBRAF cells (Supplementary Figure S9). Together, these data suggest that a high level of oncogenic BRAF, but not sustained activation of the MEK-ERK pathway, suppresses melanoma cell growth.

BRAF-induced autophagy and melanoma progression *in vivo*

To investigate the relevance of autophagy triggered by high mBRAF to melanoma growth *in vivo*, we used the mouse xenograft model. We injected vector control and 451Lu-mBRAF cells (1×10^6) into flanks of 4- to 6-week-old athymic nude mice and measured the kinetics of tumor growth. As shown in Figure 6a, mBRAF tumors grew significantly slower, and by day 40, the tumors were up to 45% smaller than the vector control tumors (two-tailed Student's *t*-test, $P = 0.03$). Kaplan–Meier analysis (percent animals surviving with a tumor volume of $\geqslant 1000\,mm^3$) showed significant difference in survival of control and 451Lu-BRAF-injected mice (Figure 6a; $P = 0.0035$ for mBRAF2 and $P = 0.0003$ for mBRAF3).

Interestingly, after 3–4 weeks of growth, most mBRAF tumors appeared red (hemorrhagic), became progressively necrotic, and showed a concave surface contour (Figure 6b and Supplementary Figure S10). At day 60, when all mice were killed, 7 of 10 mBRAF2 and 8 of 9 mBRAF3 mice showed varying levels of necrosis as scored by the surface diameter of the tumor-showing necrosis (Carswell *et al.*, 1975), whereas none (0/9) of the vector control tumor-bearing mice showed necrosis (Figure 6b and table below). Histochemical staining of the tumor sections showed robust angiotropic

growth of cells in control tumors, whereas considerable engorgement and congestion of blood vessels accompanied by hemorrhagic necrosis could be seen in mBRAF tumors with ghost cells (cell shadows) making up the bulk of the tumor (Figure 6c). Immunohistochemical analysis of LC3 showed higher expression in mBRAF tumor cells compared with vector control tumors (Figure 6c). Electron microscopy of residual mBRAF tumors showed characteristic ultrastructural features of necrosis (Figure 6d), such as irregularly condensed chromatin, breakdown of plasma membrane and organelles, and clear cytoplasm with vacuoles (Romanko *et al.*, 2004). These data suggest that activation of mBRAF induces autophagy and inhibits tumor growth in this *in vivo* mouse xenograft model.

To test whether in human melanomas expression levels of BRAF correlate with expression levels of autophagy marker LC3, we performed automated quantitative immunohistochemistry analysis (AQUA) using a tissue array consisting of primary ($n=16$) lymph node ($n=12$) and distant metastases of melanoma ($n=12$), and a representative set of human cutaneous melanoma cell lines ($n=5$). The range of AQUA signal intensities for BRAF and LC3 are shown in Table 1 and representative staining of two primary melanoma tumor cores is shown in Figure 7. Core 36 represents a tumor with low BRAF (AQUA score: 12.96) and LC3 (37.87) expression, and Core 39 represents a tumor with high BRAF (35.86) and LC3 (51.91) expression. Spearman's correlation analysis of intensity values of the three markers showed that BRAF and LC3 are significantly correlated among all melanoma samples ($r=0.591$; $P=0.002$). In contrast, expression of MAP2, a neuronal differentiation marker that we previously showed to be expressed in cutaneous melanomas (Fang *et al.*, 2001), showed no correlation with BRAF levels (Table 1). These data suggest that high levels of oncogenic BRAF correlate with expression of autophagic marker in human melanoma, implicating BRAF dosage-dependent autophagy as a determinant of melanoma tumor progression.

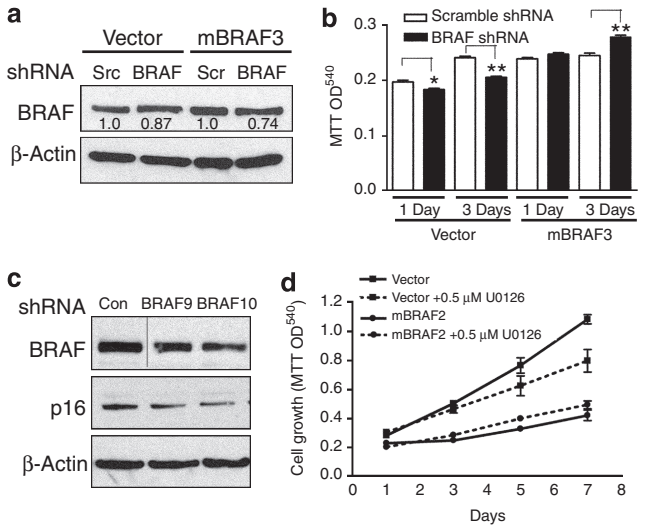

Figure 5. High levels of mBRAF are required for growth inhibition. (**a**) Partial knockdown of BRAF by shRNA lentivirus. Vector control and mBRAF cells were infected with (equal MOI) scrambled (control) and BRAF shRNA lentivirus. Transduced cells were selected by treating the cells with 1 μg ml^{-1} of puromycin for 10 days. Western blot analysis shows total BRAF protein levels in control and mBRAF cells. Actin control for equal protein loading is shown. (**b**) Partial knockdown of BRAF restores growth of 451Lu-mBRAF cells. BRAF shRNA-transduced, puromycin-selected cells were plated in a 96-well plate, and the cell growth was measured after 1 and 3 days using MTT dye. Representative data of three independent experiments are shown ($N=5$, $^*P<0.05$; $^{**}P<0.001$). (**c**) Partial knockdown of BRAF in mBRAF3 by shRNA plasmid (BRAF9 and BRAF10) transfection. Western blot analysis of total BRAF and p16 in control and BRAF shRNA-transduced cells. Actin control for equal protein loading is shown. (**d**) Inhibition MAPK signaling does not rescue growth of 451Lu-mBRAF cells. Vector control and 451Lu-mBRAF cells were treated with MEK inhibitor (0.5–10 μM, U0126) and growth was measured by MTT assay. Representative data of three experiments are shown.

DISCUSSION

In this study, we show that overexpression of BRAF^{V600E} in melanoma cells induces not only senescence-like features but also autophagy-associated growth inhibition both *in vitro* and *in vivo*. Oncogene-induced senescence and growth arrest *in vivo* are considered barriers to tumorigenesis (Prieur and Peeper, 2008) and the molecular details of oncogene-induced senescence and the mechanisms of its evasion have been extensively investigated (Wajapeyee *et al.*, 2008). The effect of different oncogene expression levels on cell fate has been investigated (Chen *et al.*, 2008). Using a regulated expression model system, it was proposed that a multistep Ras tumorigenesis model requires at least three distinct

Figure 6. Overexpression of oncogenic BRAF inhibits tumor growth and correlates with expression of autophagy marker *in vivo*. 451Lu vector control and mBRAF cells (1×10^6) were injected subcutaneously in the right flank of nu/nu athymic mice. Tumors were measured twice a week for 6 weeks in control ($n=9$), mBRAF2 ($n=10$), and mBRAF3 ($n=9$) mice. (**a**) Left: Kinetics of tumor growth shown as mean (± SEM) tumor volume (mm^3) (Two-tailed Student's *t*-test $^*P=0.03$). In all three groups, mice with the largest and smallest tumor volume were removed from the analysis. Right: Kaplan–Meier survival analysis. Percent mice that reached tumor size of 1000 mm^3 were plotted against time ($^*P=0.0035$ and $^{**}P=0.0003$). (**b**) Necrosis of mBRAF tumors. By 3–4 weeks, most 451Lu-mBRAF tumors were red (hemorrhagic) in color and became progressively necrotic (black) with a recessed or concave surface contour. Necrosis was graded (0, +1 to +3) as the surface area of the tumor showing black color, and the numbers in the table represent the number of animals with particular necrosis score at day 60. (**c**) Histology and expression of autophagy marker LC3 *in vivo*. Formalin-fixed 451Lu vector control and mBRAF tumors were sectioned and stained with hematoxylin and eosin (H&E) (bars = 4 mm; top and middle panels) and immunostained for LC3 (bar = 50 μm; bottom panel). Representative H&E and immunostained sections of a control and mBRAF tumors are shown. Arrows indicate necrosis and arrowheads show red hemorrhagic areas. (**d**) Ultrastructure of 451Lu vector control and mBRAF tumors show necrotic features in mBRAF tumors. Excised tumor tissues were fixed and processed for transmission electron microscopy. Upper panels: low magnification (bar = 5 and 10 μm for vector and mBRAF, respectively); lower panels: higher magnification (bar = 2 μm). N: nuclei; *: vacuoles, and arrowheads: plasma membrane.

oncogenic events—low level of oncogenic activation that stimulates proliferation, spontaneous upregulation of activated Ras levels that induce senescence and, finally, evasion of senescence and tumor progression (Sarkisian *et al.*, 2007). Distinct threshold levels of Myc *in vivo* also seem to determine its biological output, suggesting that low-level

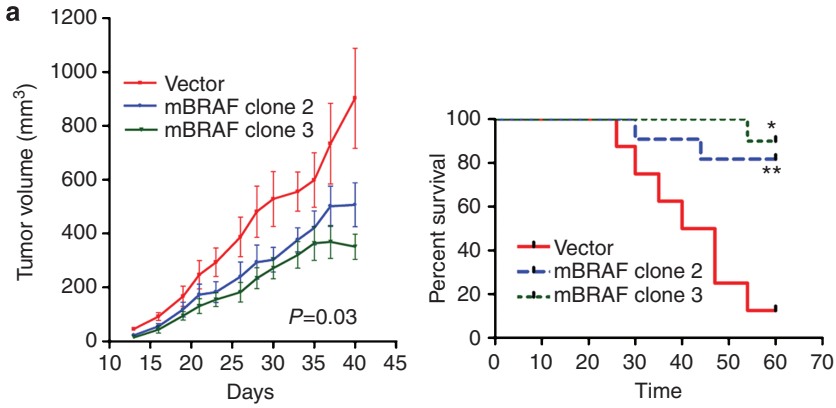

Group	–	Hemorrhagic	+	++	+++
Vector	9	0	0	0	0
mBRAF clone 2	3	1	3	1	2
mBRAF clone 3	1	0	2	4	2

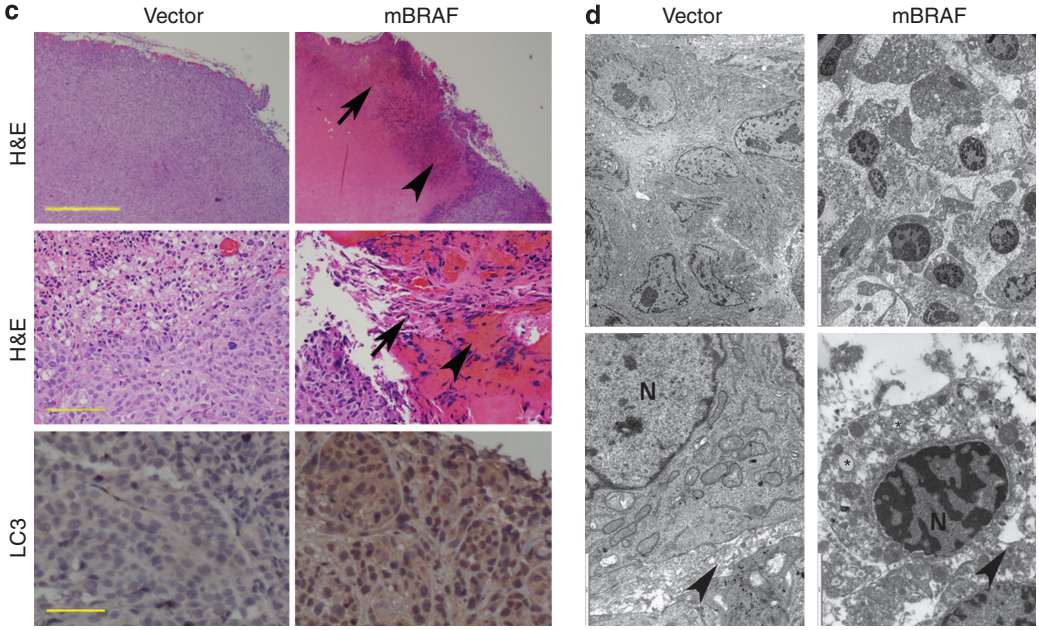

deregulated Myc may be a more efficient initiator of oncogenesis than overexpressed Myc (Murphy *et al.*, 2008). Similarly, an *in vivo* mouse model of $BRAF^{V600E}$ expression regulated by its own promoter also suggested that the distinct biological outcomes might be due to differences in the level of oncogene expression or activation (Dankort *et al.*, 2007). Our data show that overexpression of oncogenic BRAF even in highly aggressive metastatic melanoma cells harboring endogenous activated BRAF can alter their growth.

Table 1. Automated quantitative immunohistochemistry analysis (AQUA) of human melanoma tissue array

	BRAF	LC3	MAP2
n	33	26	32
Minimum	12.96	19.32	23.89
Maximum	77.51	154.2	165.6
Mean	22.39	52.48	70.11
First quartile	17.3	26.62	43.52
Third quartile	23.36	60.67	85.64

A melanoma trial tissues array (obtained from the National Cancer Institute, NIH, USA) containing primary (*n*=16), lymph node (*n*=12), and distant melanoma (*n*=12) and melanoma cell lines (*n*=5) was used for immunohistochemistry staining, and staining intensity data was acquired using AQUA. Tissues were masked with S100 antibody and stained with BRAF and LC3 and MAP2 antibody, and DAPI was used to stain the nuclei. Table shows the AQUA values of the tissues stained with BRAF, LC3, and MAP2.

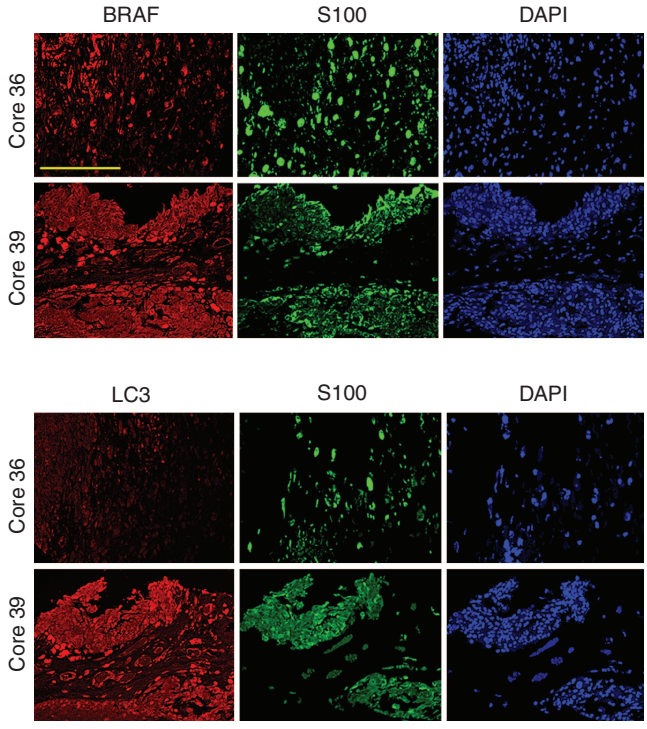

Figure 7. Automated quantitative analysis (AQUA) of human melanoma tissue array. A melanoma trial tissues array (obtained from the National Cancer Institute, NIH, USA) was used for immunofluorescent staining. The staining intensity was analyzed using AQUA. Melanoma was masked with S100 antibody and visualized with Alexa Fluor 555 (green) tagged secondary antibodies. BRAF and LC3 were stained and visualized with Alexa Fluor 647 (red) tagged secondary antibodies. 4,6-Diamidino-2-phenylindole (DAPI) was used to stain and visualize the nuclei (blue). Representative images of primary melanoma tissues stained with BRAF (upper), LC3 (lower), S100, and DAPI are shown (bar = 200 pi).

The differences in biological responses to oncogene dosage levels are highlighted by our observation that even among melanoma cell lines, the effects of overexpression of $BRAF^{V600E}$ are dependent on the endogenous activated oncogene, RAS versus. BRAF. Thus, although metastatic melanoma SK-MEL-2 cells that carry a mutation in RAS, but not in BRAF, are also susceptible to induction of senescence by mBRAF, they do not undergo proliferative arrest. This is in contrast to the observations that expression of activated N-RAS in metastatic melanoma cells harboring BRAF mutation causes growth inhibition because of cell cycle arrest in the G0/G1 phase and activation of senescence-associated markers (Petti *et al.*, 2006). Although the mutually exclusive occurrence of mutations in RAS and BRAF genes in melanoma is thought to indicate a common mechanism of action involving the downstream MEK–ERK pathway, BRAF appears to be dispensable for the RAS-activated MAPK pathway. In RAS-transformed melanocytes and melanoma cells harboring oncogenic RAS, depletion of BRAF did not block MEK–ERK signaling or cell cycle progression (Wellbrock *et al.*, 2004). In addition, although overexpression of oncogenic BRAF induces senescence, it has been suggested that it is the inactivation by the inhibitory NF1 feedback loop rather than hyperactivation of the RAS pathway that acts a senescence trigger (Courtois-Cox *et al.*, 2006). Thus, activated RAS and BRAF appear to activate common as well as distinct signaling mechanisms.

The observation that a pan-caspase inhibitor failed to rescue proliferation of mBRAF clones, together with the absence of cell cycle arrest and TUNEL-positive cells, prompted us to explore alternative cell death mechanisms. Autophagy is activated as a cell survival mechanism in response to nutrient or growth factor starvation. However, prolonged or extensive autophagy is known to contribute to cell death (Qu *et al.*, 2003; Galluzzi *et al.*, 2008). Although it has been documented that several oncogenes inhibit autophagy and tumor suppressors induce autophagy, the role of autophagy in tumor development and progression remains controversial (Maiuri *et al.*, 2008). Induction of autophagy by high $BRAF^{V600E}$ may seem contradictory to the proposed role of oncogenes, but it is consistent with the complex relationship between autophagy and tumorigenesis (Maiuri *et al.*, 2008). In NIH3T3 cells, overexpression of mutant H-Ras/Val12 has been shown to have a role in the regulation of nutrient starvation-induced autophagy through MAPK-independent pathways and through the class I PI3 kinase signaling pathway (Furuta *et al.*, 2004). However, it must be noted that in colon cancer HT29 cells, overexpression of Ras/Val12 stimulates, rather than inhibits, autophagy (Pattingre *et al.*, 2003). Thus, regulation of autophagy by oncogene overexpression appears to be cell type-specific. We show that high levels of $BRAF^{V600E}$ not only induce autophagy-associated

growth inhibition but also correlate with higher expression of autophagy marker LC3 in human melanoma tumors, suggesting a tumor-suppressive role for BRAF-induced autophagy in melanoma.

Autophagy is negatively regulated by mTOR signaling (Lum *et al.*, 2005). There are two distinct mTOR complexes, mTORC1 and mTORC2, that consist of distinct mTOR-binding proteins and also have different substrate specificities (Corradetti and Guan, 2006). We show that overexpression of mBRAF can downregulate mTOR signaling, specifically of mTORC1, which negatively regulates autophagy. On the basis of the recently published observations and our data that show an increase in the phosphorylation of mTOR on Ser2481 and an increase in Rictor, which are associated with mTORC2 (Copp *et al.*, 2009), we suggest that cross talk between BRAF and mTOR signaling has a role in determining the fates of neoplastic melanocytes. This is supported by the observation that BRAF kinase activity is inhibited by Ras homolog enriched in the brain (Rheb) that binds and regulates mTOR kinase signaling, which is reported to be upregulated in the majority of melanomas (Karbowniczek *et al.*, 2004, 2009; Long *et al.*, 2005). Recently, GOLPH3, a Golgi-located protein that modulates mTOR signaling and rapamycin sensitivity in cancer, including melanoma, has been shown to be a previously unknown oncogene supporting a role for mTOR signaling in melanoma cell survival (Scott *et al.*, 2009).

Although it has been proposed that the inhibition of autophagy could be used as the treatment of cancer, the role of autophagy in tumor progression and the benefit of induction of autophagy in cancer therapy remain to be settled (Høyer-Hansen and Jäättelä, 2008). Our data on oncogenic BRAF dosage-dependent induction of autophagy and growth inhibition in both primary and metastatic cells raises the possibility that in melanomas with activated BRAF, autophagy can serve not only as a prognostic indicator but also as an alternative cell death pathway that can be exploited for treatment.

MATERIALS AND METHODS

Cell culture

Melanoma cell lines WM115, SK-MEL-2, −28, −31, and human embryonal carcinoma cell lines, NT2/D1 and HEK293T, were purchased from American Type Culture Collection (Manassas, VA). WM35 and 451Lu melanoma cells were provided by Dr M Herlyn (Wistar Institute, Philadelphia, PA) and grown as described (Fang *et al.*, 2001). Neonatal foreskin melanocytes were isolated (Fang *et al.*, 2001) and cultured in phorbol 12-myristate 13-acetate-free medium supplemented with growth supplement (Cascade Biologics, Portland, OR).

Plasmids

BRAF expression plasmids pMCEFplink, pMCEFBRAFV600E, pEF-BRAFV600E, and pEFplink were from Dr R Marais (Institute of Cancer Research, London, UK) and pLXSP3-G $BRAF^{VE}$:ER^{T2} was from Dr M McMahon (CRI, University of California, San Francisco, CA). LC3 cDNA plasmid was from Dr N Mizushima (Tokyo University, Tokyo, Japan).

Antibodies

Anti-Raf-B, anti-MAPLC3 (Santa Cruz Biotech, Santa Cruz, CA), anti-p44/42 MAPK, anti-phospho-p44/42 MAPK (Thr202/Tyr204), anti-mTOR, anti-phospho-mTOR (Ser2448), anti-phospho-mTOR (Ser2481), anti-Raptor, anti-Rictor, anti-phospho-AKT (Thr308), anti-phospho-AKT(ser434), anti-AKT, anti-phospho-4E-BP1(Ser65), antiphospho-4E-BP1(Thr37/46), anti-4E-BP1, anti-phospho-TSC2(Thr1462), anti-TSC2 (Cell Signaling Technology, Beverly, MA), anti-p16 (Chemicon, Temecula, CA), anti-LC3 (Novus Biologicals, Littleton, CO), anti-acetyl-histone H3 (Lys9) (Upstate, Temecula, CA), and anti-β-actin antibodies were used. Horseradish peroxidase-conjugated goat anti-mouse IgG and horseradish peroxidase-conjugated donkey anti-rabbit IgG were from GE Health Care (Piscataway, NJ), and goat anti-mouse IgG Alexa 488 was from Molecular Probes (Carlsbad, CA).

Transfection

Transient transfection was performed using Lipofectamine Plus (Invitrogen, Carlsbad, CA) or NHEM-Neo Nucleofector kit (Amaxa, Gaithersburg, MD) according to the manufacturer's instructions. For stable clones, transfected 451Lu and SK-MEL-2 melanoma cells were selected and maintained in G418 ($1\,mg\,ml^{-1}$). The 451Lu ER-$BRAF^{V600E}$ stable clones were established by transfecting with pLXSP3-G $BRAF^{VE}$:ER^{T2} plasmid, selected and maintained in $1\,\mu g\,ml^{-1}$ of puromycin. SK-MEL-2 mBRAF and 451Lu-ER-BRAF stable cells represent a mixture of separate clones. In ER-$BRAF^{V600E}$ cells, BRAF was induced by adding 4-hydroxytamoxifen (Sigma, St Louis, MO).

shRNA plasmids and lentiviruses

BRAF knockdown was performed using human pLKO.1 lentiviral shRNA plasmids from the RNAi Consortium collection (Open Biosystem, Huntsville, AL). Lentiviruses were produced by transfecting scrambled control or BRAF shRNA with viral packing (pSVG) and envelope (pCMV ΔR8.2) plasmids into HEK293T cell lines. Supernatants were harvested and concentrated, and viral copy number was calculated using the quantitative reverse transcription–PCR titration kit (Clontech, Mountain View, CA). Cells were infected with an equal number of scrambled or BRAF viral particles and transduced cells were selected in medium containing $1\,\mu g\,ml^{-1}$ Puromycin.

Cell proliferation, cell death, clonogenic survival, and senescence assays

Cell growth was determined using MTT assays using 1×10^4 cells plated in a 96-well plate. MTT dye ($5\,mg\,ml^{-1}$, Sigma) was added and viable cell number (OD540) was measured. Cells (1×10^5) were cultured and on days 1, 3, and 5 were fixed in methanol and stained with 0.5% crystal violet solution in 25% methanol. Crystal violet-stained cells were solubilized in 0.1 M sodium citrate in 50% ethanol and measured (OD540). The number of dead cells was measured using the CytoTox-Glo cytotoxicity assay kit (Promega, Madison, WI) that measures dead cell protease activity. Cells (1×10^4) were plated in triplicate wells, treated with autophagy inhibitor 3-MA (Sigma), and after 24 hours cytotoxicity assay reagent ($50\,\mu l$) was added and luminescence measured. For clonogenic assay, 5×10^3 cells were cultured for 14 days, colonies were fixed, stained with 0.1% crystal violet, washed, and the colonies were counted. For senescence-associated-β-galactosidase-staining, cells plated in triplicate for

72 hours were fixed, incubated with X-gal (5-bromo-4-chloro-3-indolyl-βD-galactopyranoside) (Cell Signaling) at 37 °C overnight, observed under a microscope for the development of blue color, and photographed. Cells stained blue were counted and percent stained cells were estimated.

Cell cycle and apoptosis assays

Apoptotic cells were detected using the Apo-Direct apoptosis detection kit (Phoenix Flow System, San Diego, CA). Cells were fixed and the DNA breaks in the cells undergoing apoptosis were labeled with TdT and FITC-dUTP and scanned by flow cytometry. Propidium iodide staining was performed by incubating the cells with propidium iodide and cell cycle was analyzed by flow cytometry.

GFP–LC3 staining

Autophagic vacuoles were identified using GFP–LC3 plasmid transfection (Kabeya *et al.*, 2000). Cells on glass coverslips were transfected with pEGFP-LC3 plasmid for 24 hours, fixed in paraformaldehyde, washed, and mounted and images were captured using the Bio-Rad Radiance 2100 MP Rainbow (Hercules, CA) confocal microscope.

Immunoblotting

Cells cultured under the indicated conditions were lysed in 1% Triton X-100 in phosphate-buffered saline, or in RIPA buffer containing sodium vanadate (Sigma) and a cocktail of protease inhibitors (Roche Diagnostics, Indianapolis, IN). Protein was estimated using the BCA protein assay kit (Pierce Biotechnology, Rockford, IL), separated by SDS–PAGE, and transferred to a Polyscreen membrane (Perkin Elmer Life Sciences, Boston, MA). Membranes were blocked with 5% non-fat dry milk and incubated overnight at 4 °C with primary antibodies. The blots were incubated in appropriate horseradish peroxidase-conjugated secondary antibody and proteins were detected by chemiluminescence (Amersham Biosciences, Piscataway, NJ). β-Actin was used as a control to monitor protein loading variability.

Immunofluorescence and immunohistochemistry

Cells on coverslips were fixed in paraformaldehyde, permeabilized with cold methanol, incubated with LC3 antibody (Santa Cruz), and washed and the bound antibody was visualized using Alexa Fluor 488 (green)-conjugated secondary antibody. Nuclei were stained with propidium iodide and images were acquired using a confocal microscope. Immunohistochemistry was performed on sections of formalin-fixed paraffin-embedded mouse tumors and human melanoma tumors using the Histostain-plus kit (Zymed, San Francisco, CA) according to the manufacturer's manual. Antigen retrieval was performed by heating in a microwave for 20 minutes in citrate buffer, pH 6.0. Endogenous peroxidase quenching was performed using 3% H_2O_2. Tissue sections were incubated in primary antibody, washed and incubated in biotinylated secondary antibody followed by horseradish peroxidase-conjugated streptavidin and chromogen AEC, counterstained with hematoxylin, and observed on a Nikon phase contrast microscope (Melville, NY).

Transmission electron microscopy

Cells on coverslips were washed with phosphate-buffered saline, fixed with 2.5% glutaraldehyde, and processed for transmission electron microscopy. Ultrathin sections were observed and photographed using the Jeol 100 electron microscope (Tokyo, Japan) at the UW Electron Microscope Facility.

Mouse xenograft

Athymic Ncr-nu/nu mice (4–6 weeks, male and female) were purchased from the National Cancer Institute (NCI, Frederick, MD). 451Lu mBRAF and vector control cells (1×10^6) were injected subcutaneously into the right flanks. Tumor size was measured every third day using digital calipers and photographed. All animal experiments were approved by and carried out according to IACUC guidelines.

Automated quantitative analysis

Human melanoma tissue arrays (Mini Test Array, NCI, USA) consisting of primary lymph node and distant metastatic melanomas and melanoma cell lines were used to quantify the expression of BRAF, LC3, and MAP2 by AQUA as described (Warren *et al.*, 2009). Anti-S100 protein (Biocare Medical, Concord, CA) and Alexa Fluor 555 tagged secondary antibody was used as the melanoma tumor mask. BRAF, LC3, and MAP2 were visualized with Alexa Fluor 647-tagged secondary antibodies. Nuclei were stained with 4,6-diamidino-2-phenylindole. Details of the image acquisition and pixel quantitation analysis are described in Supplementary Data.

Statistical analysis

Data were analyzed using Prizm 4.0 (GraphPad Software, La Jolla, CA). Mouse tumor data were analyzed using two-tailed *t*-test and all other data were analyzed using one-way analysis of variance. AQUA data were analyzed using Pearson's correlation analysis.

CONFLICT OF INTEREST

The authors state no conflict of interest.

ACKNOWLEDGMENTS

This study was supported in part by the National Institutes of Health Grant R21CA125091 to VS.

SUPPLEMENTARY MATERIAL

Supplementary material is linked to the online version of the paper at http://www.nature.com/jid

REFERENCES

Braig M, Schmitt CA (2006) Oncogene-induced senescence: putting the brakes on tumor development. *Cancer Res* 66:2881–4

Carswell EA, Old LJ, Kassel RL *et al.* (1975) An endotoxin-induced serum factor that causes necrosis of tumors. *Proc Natl Acad Sci USA* 72:3666–70

Chen W, Kumar AR, Hudson WA *et al.* (2008) Malignant transformation initiated by Mll-AF9: gene dosage and critical target cells. *Cancer Cell* 13:432–40

Copp J, Manning G, Hunter T (2009) TORC-specific phosphorylation of mammalian target of rapamycin (mTOR): phospho-Ser2481 is a marker for intact mTOR signaling complex 2. *Cancer Res* 69:1821–7

Corradetti MN, Guan KL (2006) Upstream of the mammalian target of rapamycin: do all roads pass through mTOR? *Oncogene* 25: 6347–60

Courtois-Cox S, Williams SMG, Reczek EE *et al.* (2006) A negative feedback signaling network underlies oncogene-induced senescence. *Cancer Cell* 10:459–72

Dankort D, Curley DP, Cartlidge RA *et al.* (2009) BrafV600E cooperates with Pten loss to induce metastatic melanoma. *Nature Genetics* 41:544–52

Dankort D, Filenova E, Collado M *et al.* (2007) A new mouse model to explore the initiation, progression, and therapy of BRAFV600E-induced lung tumors. *Genes Dev* 21:379–84

Davies H, Bignell GR, Cox C *et al.* (2002) Mutations of the BRAF gene in human cancer. *Nature* 417:949–54

Demunter A, Stas M, Degreef H *et al.* (2001) Analysis of N- and K-Ras mutations in the distinctive tumor progression phases of melanoma. *J Invest Dermatol* 117:1483–9

Dumaz N, Hayward R, Martin J *et al.* (2006) In melanoma, RAS mutations are accompanied by switching signaling from BRAF to CRAF and disrupted cyclic AMP signaling. *Cancer Res* 66:9483–91

Eisen T, Ahmad T, Flaherty KT *et al.* (2006) Sorafenib in advanced melanoma: a Phase II randomised discontinuation trial analysis. *Br J Cancer* 95:581–6

Fang D, Hallman J, Sangha N *et al.* (2001) Expression of microtubule-associated protein 2 in benign and malignant melanocytes: implications for differentiation and progression of cutaneous melanoma. *Am J Pathol* 158:2107–15

Furuta S, Hidaka E, Ogata A *et al.* (2004) Ras is involved in the negative control of autophagy through the class I PI3-kinase. *Oncogene* 23:3898–904

Galluzzi L, Morselli E, Vicencio JM *et al.* (2008) Life, death and burial: multifaceted impact of autophagy. *Biochem Soc Trans* 036:786–90

Hoeflich KP, Gray DC, Eby MT *et al.* (2006) Oncogenic BRAF is required for tumor growth and maintenance in melanoma models. *Cancer Res* 66:999–1006

Høyer-Hansen M, Jäättelä M (2008) Autophagy. An emerging target for cancer therapy. *Autophagy* 4:574–80

Kabeya Y, Mizushima N, Ueno T *et al.* (2000) LC3, a mammalian homologue of yeast Apg8p, is localized in autophagosome membranes after processing. *EMBO J* 19:5720–8

Karbowniczek M, Cash T, Cheung M *et al.* (2004) Regulation of B-Raf kinase activity by tuberin and Rheb is mammalian target of rapamycin (mTOR)-independent. *J Biol Chem* 279:29930–7

Karbowniczek M, Spittle CS, Morrison T *et al.* (2009) mTOR is activated in the majority of malignant melanomas. *J Invest Dermatol* 128:980–7

Karreth FA, DeNicola GM, Winter SP *et al.* (2009) C-Raf inhibits MAPK activation and transformation by B-RafV600E. *Mol Cell* 36:477–86

Long X, Lin Y, Ortiz-Vega S *et al.* (2005) Rheb binds and regulates the mTOR kinase. *Curr Biol* 15:702–13

Lum JJ, DeBerardinis RJ, Thompson CB (2005) Autophagy in metazoans: cell survival in the land of plenty. *Nat Rev Mol Cell Biol* 6:439–48

Maiuri MC, Tasdemir E, Criollo A *et al.* (2008) Control of autophagy by oncogenes and tumor suppressor genes. *Cell Death Differ* 16:87–93

Michaloglou C, Vredeveld LC, Soengas WMS *et al.* (2005) BRAFE600-associated senescence-like cell cycle arrest of human naevi. *Nature* 436:720–4

Murphy DJ, Junttila MR, Pouyet L *et al.* (2008) Distinct thresholds govern Myc's biological output *in vivo*. *Cancer Cell* 14:447–57

Pattingre S, Bauvy C, Codogno P (2003) Amino acids interfere with the ERK1/2-dependent control of macroautophagy by controlling the activation of Raf-1 in human colon cancer HT-29 cells. *J Biol Chem* 278: 16667–74

Patton EE, Widlund HR, Kutok JL *et al.* (2005) BRAF mutations are sufficient to promote nevi formation and cooperate with p53 in the genesis of melanoma. *Curr Biol* 15:249–54

Petiot A, Ogier-Denis E, Blommaart EFC *et al.* (2000) Distinct classes of phosphatidylinositol 3′-kinases are involved in signaling pathways that control macroautophagy in HT-29 cells. *J Biol Chem* 275: 992–8

Petti C, Molla A, Vegetti C *et al.* (2006) Coexpression of NRASQ61R and BRAFV600E in human melanoma cells activates senescence and increases susceptibility to cell-mediated cytotoxicity. *Cancer Res* 66: 6503–11

Prieur A, Peeper DS (2008) Cellular senescence *in vivo*: a barrier to tumorigenesis. *Curr Opin Cell Biol* 20:150–5

Qu X, Yu J, Bhagat G *et al.* (2003) Promotion of tumorigenesis by heterozygous disruption of the beclin 1 autophagy gene. *J Clin Invest* 112:1809–20

Romanko MJ, Rothstein RP, Levison SW (2004) Neural stem cells in the subventricular zone are resilient to hypoxia/ischemia whereas progenitors are vulnerable. *J Cerebral Blood Flow Metab* 24:814–25

Sarkisian CJ, Keister BA, Stairs DB *et al.* (2007) Dose-dependent oncogene-induced senescence *in vivo* and its evasion during mammary tumorigenesis. *Nat Cell Biol* 9:493–505

Scott KL, Kabbarah O, Liang M-C *et al.* (2009) GOLPH3 modulates mTOR signalling and rapamycin sensitivity in cancer. *Nature* 459: 1085–90

Sensi M, Nicolini G, Petti C *et al.* (2006) Mutually exclusive NRASQ61R and BRAFV600E mutations at the single-cell level in the same human melanoma. *Oncogene* 25:3357–64

Serrano M, Lin AW, McCurrach ME *et al.* (1997) Oncogenic *ras* provokes premature cell senescence associated with accumulation of p53 and p16INK4a. *Cell* 88:593–602

Solit DB, Garraway LA, Pratilas CA *et al.* (2006) BRAF mutation predicts sensitivity to MEK inhibition. *Nature* 439:358–62

Turcotte S, Chan DA, Sutphin PD *et al.* (2008) A molecule targeting VHL-deficient renal cell carcinoma that induces autophagy. *Cancer Cell* 14:90–102

Uribe P, Andrade L, Gonzalez S (2006) Lack of association between BRAF mutation and MAPK ERK activation in melanocytic nevi. *J Invest Dermatol* 126:161–6

Wajapeyee N, Serra RW, Zhu X *et al.* (2008) Oncogenic BRAF induces senescence and apoptosis through pathways mediated by the secreted protein IGFBP7. *Cell* 132:363–74

Warren M, Twohig M, Pier T *et al.* (2009) Protein expression of matriptase and its cognate inhibitor HAI-1 in human prostate cancer: a tissue microarray and automated quantitative analysis. *Appl Immunohistochem Mol Morphol* 17:23–30

Wellbrock C, Ogilvie L, Hedley D *et al.* (2004) V599EB-RAF is an oncogene in melanocytes. *Cancer Res* 64:2338–42